

High-Energy K^- -Meson Interactions and Decays*

STANLEY C. FREDEN, FRANCIS C. GILBERT, AND R. STEPHEN WHITE
Lawrence Radiation Laboratory, University of California, Livermore, California

(Received October 20, 1959)

The interactions of 20 to 300 Mev K^- mesons on free protons and on emulsion nuclei have been studied and their decays analyzed. The K^- -meson mean lifetime is found to be $(1.38 \pm 0.24) \times 10^{-8}$ sec. Examples of the decay modes $K_{\mu 2}$, $K_{\pi 2}$, $K_{\mu 3}$, τ , and τ' are identified. The branching ratios are found to be in agreement with those for K^+ mesons. The (K^-p, K^-p) elastic scattering cross section is found to be 35 ± 16 mb and the $(K^-p, \Sigma^{\pm}\pi^{\mp})$ cross section 27 ± 13 mb in the energy region of 150 to 300 Mev. The mean free path for K^- -meson captures and inelastic scatters on emulsion nuclei, except hydrogen, can be represented by $\Lambda(\text{cm}) = (17.2 \pm 3.4) + (0.081 \pm 0.027)T_K$, where T_K is the laboratory K^- -meson kinetic energy, for K^- -meson energies from 20 to 300 Mev. This increase in the mean free path with K^- -meson energy is explained in terms of the decreasing nucleon cross section. The fraction of the interactions of K^- mesons on nuclei which are inelastic scatters increases from 2% at low K^- -meson energies to about 15% at 150 Mev. This increase in inelastic scattering with energy is additional evidence that the nucleus is becoming partially transparent to K^- mesons at about 150 Mev. Data are presented for the fraction of events with observed π mesons, Σ hyperons, and π meson- Σ hyperon pairs. The data are discussed in terms of the model which was previously presented to explain K^- meson captures at rest on nucleons bound in nuclei.

I. INTRODUCTION

RECENTLY a large amount of information has been published concerning K^- -meson decays and interactions. Most of this has come from experiments which were performed with emulsion stacks¹⁻¹⁴ or with bubble chambers¹⁵⁻¹⁷ at the Berkeley bevatron.

* Work was performed under the auspices of the U. S. Atomic Energy Commission.

¹ F. C. Gilbert, C. E. Violet, and R. S. White, Phys. Rev. **103**, 1825 (1956).

² W. Alles, N. N. Biswas, M. Ceccarelli, and J. Crussard, Nuovo cimento **6**, 571 (1957). W. Alles, N. N. Biswas, M. Ceccarelli, R. Gessaroli, G. Quareni, H. Göing, K. Gottstein, W. Püschel, J. Tietge, G. T. Zorn, J. Crussard, J. Hennessy, G. Dascola, and S. Mora, Nuovo cimento **11**, 771 (1959).

³ R. G. Glasser, N. Seeman, and G. A. Snow, Nuovo cimento **7**, 142 (1958), and Nuovo cimento **9**, 1085 (1958).

⁴ E. Lohrmann, M. Nikolić, M. Schneeberger, P. Waloschek, and H. Winzeler, Nuovo cimento **7**, 163 (1958).

⁵ G. L. Bacchella, A. Berthelot, A. Bonetti, O. Goussu, F. Lévy, M. René, D. Revel, J. Sacton, L. Scarsi, G. Tagliaferri, and G. Vanderhaeghe, Nuovo cimento **8**, 215 (1958).

⁶ Y. Eisenberg, W. Koch, E. Lohrmann, M. Nikolić, M. Schneeberger, and H. Winzeler, Nuovo cimento **8**, 663 (1958).

⁷ F. H. Webb, E. L. Iloff, F. H. Featherston, W. W. Chupp, G. Goldhaber, and S. Goldhaber, Nuovo cimento **8**, 899 (1958).

⁸ J. Hornbostal and G. T. Zorn, Phys. Rev. **109**, 165 (1958).

⁹ Y. Eisenberg, W. Koch, E. Lohrmann, M. Nikolić, M. Schneeberger, and H. Winzeler, Nuovo cimento **9**, 745 (1958).

¹⁰ Y. Eisenberg, W. Koch, M. Nikolić, M. Schneeberger, and H. Winzeler, Nuovo cimento **11**, 351 (1959).

¹¹ G. Ascoli, R. D. Hill, and T. S. Yoon, Nuovo cimento **9**, 813 (1958).

¹² Bhowmik, Evans, Falla, Hassan, Kamal, Nagpaul, Prowse, M. René, Alexander, Johnston, O'Ceallaigh, Keefe, Burhop, Davis, Kumar, Lasich, Skaukat, Stannard, G. L. Bacchella, Bonetti, Dilworth, Occhialini, L. Scarsi, Grilli, Guerriero, von Lindern, Merlin, and Salandin (to be published).

¹³ G. B. Chadwick, S. A. Durrani, P. B. Jones, J. W. G. Wignall, and D. H. Wilkinson, Phil. Mag. **3**, 1193 (1958).

¹⁴ W. H. Barkas, N. N. Biswas, D. A. DeLise, J. N. Dyer, H. H. Heckman, and F. M. Smith, Phys. Rev. Letters **2**, 466 (1959).

¹⁵ L. W. Alvarez, H. Bradner, P. Falk-Vairant, J. D. Gow, A. H. Rosenfeld, F. T. Solmitz, and R. D. Tripp, Nuovo cimento **5**, 1026 (1957). A. Rosenfeld, *Proceedings of the Seventh Annual Rochester Conference on High-Energy Nuclear Physics, 1957* (Interscience Publishers, Inc., New York, 1957), Session VIII.

¹⁶ P. Nordin, Bull. Am. Phys. Soc. **3**, 336 (1958). A. Rosenfeld,

Hydrogen bubble chamber data have been obtained up to 140 Mev. Most of the emulsion data are below 90 Mev. The Berne group^{6,9,10} has extended the K^- -energy data from emulsions to 150 Mev. An additional point for the K^-p total cross section has been measured with scintillation detectors at 530 Mev.¹⁸ Data at 760 Mev¹⁴ and at 960 and 1230 Mev¹⁹ have recently been published. In the present experiment, data for K^- -meson interactions are presented for the heretofore unexplored K^- -meson energy region of 150 to 300 Mev. Data are also added to the K^- -energy interval from 20 to 150 Mev and the published data have been collected and summarized.

Data from K^- decays and a discussion of the K^- -lifetime and decay modes are presented in Sec. 2. Data from K^- captures and scatters in flight on free protons and a discussion of the (K^-p, K^-p) and $(K^-p, \Sigma\pi)$ cross sections as a function of the K^- -meson energy are given in Sec. 3. The data for K^- -meson inelastic scattering and capture by emulsion nuclei are given in Sec. 4 and the model previously presented to explain K^- captures at rest by nuclei²⁰⁻²² is extended to explain these data.

The K^- mesons were obtained from focused and separated beams at the Berkeley bevatron which have been previously described.^{1,21,22} The 300-Mev K^- mesons

Bull. Am. Phys. Soc. **3**, 363 (1958). P. Nordin, A. H. Rosenfeld, F. T. Solmitz, R. D. Tripp, and M. B. Watson, Bull. Am. Phys. Soc. **4**, 288 (1959).

¹⁷ N. Horwitz, D. Miller, J. J. Murray, M. Schwartz, and H. D. Taft, Bull. Am. Phys. Soc. **3**, 363 (1958). N. Horwitz, D. Miller, and J. J. Murray, Bull. Am. Phys. Soc. **4**, 289 (1959).

¹⁸ B. Cork, G. R. Lambertson, O. Piccioni, and W. A. Wenzel, Phys. Rev. **106**, 167 (1957).

¹⁹ H. C. Burrows, D. O. Caldwell, D. H. Frisch, D. A. Hill, D. M. Ritson, and R. A. Schluter, Phys. Rev. Letters **2**, 117 (1959).

²⁰ Richard Capps, Phys. Rev. **107**, 239 (1957).

²¹ F. C. Gilbert, C. E. Violet, and R. S. White, Phys. Rev. **107**, 228 (1957).

²² F. C. Gilbert and R. S. White, Phys. Rev. **109**, 1770 (1958).

presented a specific problem as their ionization, relative to plateau, was only 1.3 at pickup, a position about 1 cm in from the edge of the stack. A prospective K^- meson was picked from the background of 300 minimum tracks per K^- by inspection and a count of 200 blobs was made. If the blob density was appropriate to a K^- meson an additional 800 blobs were counted before accepting the track. All the data for the interactions and decays in flight were obtained from "along the track scanning" with the exception of five decays in flight which were found by area scanning (see Sec. 2). The usual methods of ionization²³ versus range, change in ionization versus change in range, ionization versus multiple scattering, and prong endings were used for identification of the particles emitted from the K^- interactions and decays.

2. DECAYS IN FLIGHT

Thirty-five decays in flight were found by "along the track" scanning. An additional five were found by area scanning and are included in the analysis of the decay modes but not in the lifetime calculation. Any possible decay which had a blob, slow electron, or recoil was rejected. Interactions in flight were eliminated statistically by estimating the number that look like decays. The ratio of pseudo decay-like events, each of which consists of a light meson plus blob, electron, or recoil, to decay-like events among K^- -meson captures at rest is about 3 to 1. Four pseudo decay-like events were observed among the possible decays in flight. We therefore estimate that one decay-like interaction has been erroneously included among the decays in flight.

The properties of the forty decays in flight are listed in Table I. The first column gives the event number. The second column gives the observed decay product as determined by its characteristic interaction or decay. A light track which did not come to rest in the emulsion is labelled "l.t.". The secondaries from events 645, 2216, and 2197 are identified as π mesons from their interactions in flight. The third column lists the most probable decay mode. The fourth column lists the energy of the K^- meson at the decay point as determined by the better of two methods: (1) ionization or (2) known energy at entrance into the stack minus energy loss to the point of decay. The last column gives the center-of-mass angle of the light particle which was obtained from the laboratory angle, the K^- -meson energy and, where appropriate, an ionization measurement of the velocity of the secondary. The center-of-mass angle determined in this fashion is independent of the decay mode. The experimental center-of-mass angular distribution of the negatively charged secondaries is consistent with isotropy.

A. Decay Modes

Because of the high energies of the secondary particles from the K^- decays in flight, few of them

TABLE I. List of K^- -meson decay events.

Event number	Decay product	Most probable decay mode	K^- energy at decay point (Mev)	Center-of-mass angle between K^- meson and its light decay particle (deg)
14	l.t.	$K_{\mu 2}$	16	53
31	l.t.	$K_{\pi 2}$	70	102
37	l.t.	$K_{\mu 2}$	37	62
90	l.t.	unidentified	107	147
135	l.t.	$K_{\pi 2}$	79	113
359	l.t.	$K_{\mu 2}$	24	31
404	l.t.	$K_{\mu 2}$	61	91
570	l.t.	$K_{\mu 2}$	83	139
585	l.t.	unidentified	48	67
612	$\pi^-(\sigma_2)$	$K_{\pi 2}$	86	118
641	l.t.	$K_{\mu 2}$	30	82
645	π^- (l.t. interacts in flight)	$K_{\pi 2}$	30	69
667	l.t.	$K_{\mu 2}$	50	58
685	l.t.	$K_{\pi 2}$	109	82
765	l.t.	unidentified	111	63
1202	l.t.	$K_{\mu 2}$	37	37
1320	$\pi^-(\sigma_3) + e^+ + e^-$	$K_{\pi 3}(\tau')$	102	144
1339	l.t.	$K_{e 3}$ (possible $K^- IIF$)	133	153
1451	l.t.	unidentified	35	94
2006	$\mu^- \rightarrow e^-$	$K_{\mu 2}$	205	147
2053	$\left\{ \begin{array}{l} \pi^+ \rightarrow \mu^+ \rightarrow e^+ \\ \pi^-(\sigma_1) \\ \pi^-(\rho) \end{array} \right.$	$K_{\pi 3}(\tau)$	165	...
2109	$\mu^-(\sigma_1)$	$K_{\mu 3}$	262	141
2054	l.t.	$K_{\mu 2}$	112	125
2091	l.t.	$K_{\mu 2}$	44	95
2036	l.t.	$K_{\mu 2}$	66	120
2038	$\mu^-(\rho)$	$K_{\mu 2}$	245	154
5072 ^a	$\mu^- \rightarrow e^-$	$K_{\mu 3}$	<20	110
6153 ^a	l.t.	unidentified	<20	96
2134	l.t.	$K_{\mu 2}$	229	113
2153	l.t.	$K_{\pi 2}$	79	46
6191 ^a	l.t.	unidentified	<20	74
2216	π^- (l.t. interacts in flight)	$K_{\pi 2}$	122	12
2284	l.t.	unidentified	170	55
7687 ^a	$\mu^-(\rho)$	$K_{\mu 3}$	<20	90
2276	l.t.	unidentified	174	79
7863 ^a	l.t.	$K_{\pi 2}$	<20	54
2197	$\pi^-(\rho)$ (inelastic scatter in flight)	$K_{\pi 2}$	243	124
2308	l.t.	unidentified	290	88
2161	l.t.	$K_{\mu 2}$	162	120
2261	l.t.	unidentified	200	63

^a Found by area scanning.

stopped in the stacks. For those two-particle decays where the charged secondary stops the identification of the decay mode is well established from the kinematics. In some cases where the secondaries did not stop the conditions were sufficiently favorable for ionization or multiple scattering measurements to permit identification of the decay modes. Since all the well identified decays are compatible with the known decay modes²⁴ of K^+ mesons, the events are categorized according to these modes.

(a) $K_{\mu 2}$ —there were two decays which unambiguously fell into this category. In event 2006 a light

²³ P. H. Fowler and D. H. Perkins, Phil. Mag. 46, 587 (1955).

²⁴ R. W. Birge, D. H. Perkins, J. R. Peterson, D. H. Stork, and M. N. Whitehead, Nuovo cimento 4, 834 (1956).

meson came to rest in the emulsion and decayed into an electron. In event 2038 a light meson came to rest in a zero-pronged star. The kinematics of both events fit the $K_{\mu 2}$ -decay mode only.

(b) $K_{\pi 2}$ —one event, 612, clearly fits the $K_{\pi 2}$ -decay mode. The light meson ended in a two-pronged star. In addition, events 645, 2216, and 2197 are identified as $K_{\pi 2}$ decays because the light mesons interacted in flight and the kinematics are compatible with the $K_{\pi 2}$ -decay mode.

(c) $K_{\pi 3}$ —two examples of this decay mode were seen. In event 2053 three light mesons were identified, the first ended in a $\pi^+\mu^+e^+$ decay, the second in a zero-pronged star, and the third in a one-pronged star. The kinematics fit a $K_{\pi 3}$. An example of a τ' decay, event 1320, was also observed. One light meson which ended in a three-pronged star and two electrons were observed from the K^- -decay point. This event has been described in detail elsewhere.²⁵

(d) $K_{\mu 3}$ —three events clearly fall into this category. The light particles from events 2109, 5072, and 7687 ended, respectively, in a one-pronged star, an electron decay and a zero-pronged star. The kinematics of all three events are compatible only with the $K_{\mu 3}$ mode of decay.

(e) $K_{e 3}$ —no clearly identifiable decays via this mode were seen. Event 1339 has been placed in this category as it will fit no other decay mode. It may instead be a K^- interaction in flight.

The remaining 28 events each have only 1 charged prong which rules out τ decays. The momentum-versus-decay angle for these events also rules out τ' decays. The possibility of electron secondaries has been eliminated for most of these events by the change in scattering versus change in range. $K_{\mu 3}$ decays cannot be ruled out for many of these events; however, since the μ meson from the $K_{\mu 3}$ usually has a low momentum these events are not likely to be confused with the $K_{\mu 2}$ and $K_{\pi 2}$ decay modes. Therefore, an attempt was made to separate the remaining 28 events into these two latter categories by multiple scattering and ionization measurements. 13 were found to be compatible with the $K_{\mu 2}$ decay mode, 5 with the $K_{\pi 2}$, and 10 were compatible with both.

If the remaining 10 unidentified events are divided among the $K_{\mu 2}$ and $K_{\pi 2}$ decay modes in the observed ratio of 13 to 5, one arrives at the frequencies listed in Table II. Also listed are the relative frequencies for the K^+ mesons.²⁴ From the table it can be seen that the probabilities of occurrence of the various decay modes of the K^- meson are the same, within experimental uncertainties, as those of the K^+ meson.

B. K^- -Meson Lifetime

The K^- -meson mean lifetime was obtained by dividing the total observed K^- -meson proper time by

²⁵ S. C. Freden, F. C. Gilbert, and R. S. White, Phys. Rev. Letters 1, 217 (1958).

the number of decays. Thirty-five decay-like events were found by along-the-track scanning. One false decay expected from a K^- -meson interaction in flight and one event below the 2-mm residual range cutoff imposed to eliminate interactions at rest were subtracted to give 33 K^- -meson decays. Each K^- -meson stop-in-flight event was carefully examined for light prongs by three different observers at different times. In order to estimate the fraction of light tracks missed, each of the three observers looked at 65 μ^+ endings from $\pi^+\mu^+$ decays at rest. No electrons were missed. The scanning efficiency for decay prongs thus approaches 100%. The resulting K^- -meson mean lifetime is $(1.38 \pm 0.24) \times 10^{-8}$ sec. This is in agreement with the lifetimes of $(0.95_{-0.25}^{+0.36})$,²⁶ (1.60 ± 0.3) ,⁶ (1.25 ± 0.11) ²⁷ and (1.17 ± 0.12) ¹⁹ $\times 10^{-8}$ sec which have been previously reported. It is also statistically the same as the K^+ -meson lifetime of $(1.24 \pm 0.02) \times 10^{-8}$ sec.²⁸

3. FREE PROTON INTERACTIONS

The following reactions of K^- mesons on free protons are permitted by conservation of baryons, charge, and strangeness.

$$K^- + p \rightarrow \Sigma^- + \pi^+ \quad (1)$$

$$\rightarrow \Sigma^+ + \pi^- \quad (2)$$

$$\rightarrow \Sigma^0 + \pi^0 \quad (3)$$

$$\rightarrow \Lambda^0 + \pi^0 \quad (4)$$

$$\rightarrow K^- + p \quad (5)$$

$$\rightarrow \bar{K}^0 + n. \quad (6)$$

In nuclear emulsions, reactions (1), (2), and (5) are easily separated from interactions on nuclei because the

TABLE II. Frequency of decay modes of K^- mesons.

Decay mode	Well			Total	Decay percentages	
	iden- tified ^a	Iden- tified ^b	Inferred ^c		K^-	K^+ ^d
$K_{\mu 2}$	2	13	7	22	55_{-14}^{+18}	(58.5 ± 3.0)
$K_{\pi 2}$	4	5	3	12	30_{-10}^{+14}	(27.7 ± 2.7)
τ	1	0	0	1	3_{-3}^{+7}	(5.56 ± 0.44)
τ'	1	0	0	1	3_{-3}^{+7}	(2.15 ± 0.47)
$K_{\mu 3}$	3	0	0	3	7_{-4}^{+8}	(2.83 ± 0.95)
$K_{e 3}$	0	1	0	1	3_{-3}^{+7}	(3.23 ± 1.30)

^a The secondary stopped or interacted in the emulsion for each of these events.

^b These events were identified by multiple scattering, and/or ionization (see text).

^c These events were not identified. They were assigned to $K_{\mu 2}$ and $K_{\pi 2}$ in the same ratio as the "identified" events.

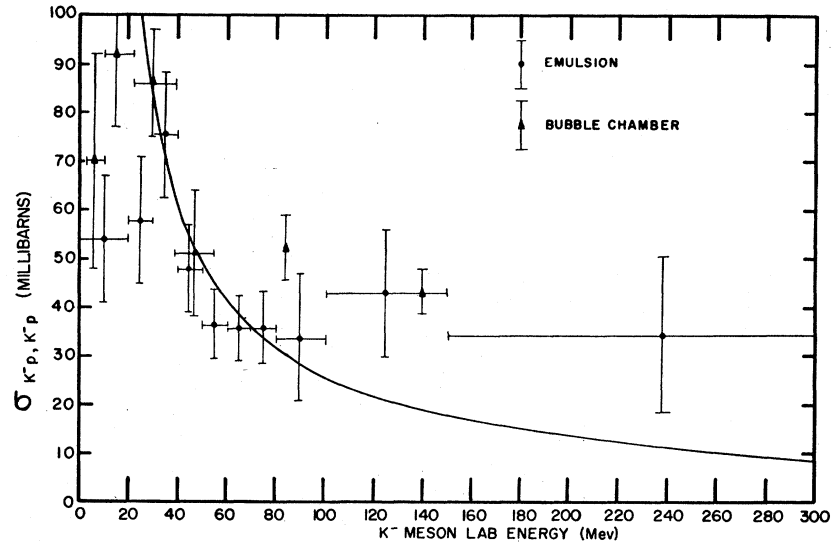
^d See reference 24.

²⁶ E. L. Iloff, G. Goldhaber, S. Goldhaber, J. E. Lannutti, F. C. Gilbert, C. E. Violet, R. S. White, D. M. Fournet, A. Pevsner, D. Ritson, and M. Widgoff, Phys. Rev. 102, 927 (1956).

²⁷ Walter H. Barkas, *Proceedings of the Seventh Annual Rochester Conference on High-Energy Nuclear Physics, 1957* (Interscience Publishers, Inc., New York, 1957), Chap. VIII.

²⁸ Frank Crawford, *Proceedings of the Seventh Annual Rochester Conference on High-Energy Nuclear Physics, 1957* (Interscience Publishers, Inc., New York, 1957).

FIG. 1. Plot of the published data for the K^- -meson free proton cross sections versus the K^- -meson laboratory kinetic energy. Superimposed on the data is the curve for $\pi\lambda^2$, where λ is the K^- -meson wavelength in the center-of-mass system divided by 2π .



following conditions must be satisfied for each event: (1) coplanarity, (2) conservation of energy, (3) conservation of longitudinal momentum, and (4) conservation of transverse momentum. For K^-p scattering, the energies and angles of both the scattered K^- meson and the proton can usually be measured very accurately. From the position in the stack and g^* measurements on the incoming K^- -meson track a good estimate of the incident K^- -meson energy can be obtained. The problem is overdetermined and several checks are available. Furthermore, below 150-MeV inelastic scattering accounts for only about 2% of the events and consequently there is no background to simulate free

proton scattering. Although inelastic scattering occurs in 20% of the events at energies above 150 MeV none were observed that come close to satisfying the conditions for a free proton scatter. For the production reactions ($K^-p, \Sigma\pi$) the situation is almost as clearcut. The above mentioned conditions apply. The Σ -hyperon and π -meson angles relative to the K^- meson, and the Σ -hyperon energy can usually be measured very accurately. If the π meson comes to rest in the stack, its energy can be precisely measured. If it escapes from the stack or interacts in flight, a g^* measurement near where it escapes or interacts can be used to obtain its energy. Again the kinematics are overdetermined so that checks can be made. The background of $\Sigma\pi$ pairs from bound protons is low because, contrary to what is observed from K^- captures at rest, most $\Sigma\pi$ events from K^- captures in flight on nuclei have one or more additional prongs. Again there is essentially no background to simulate free proton events.

The K^- -meson free proton scattering events are listed in Table III and the K^- -meson free proton capture events are listed in Table IV. The K^- -meson scattering angle, θ , in the center-of-mass system and the incident K^- -meson kinetic energy are also given in Table III. The π -meson production angle in the center-of-mass system, the incident K^- -meson kinetic energy and the identification of the Σ hyperon are also given in Table IV.

The data of the Gottingen,² Naval Research Laboratory,³ Bern,⁴ Urbana,¹¹ and K^- -stack collaboration¹² emulsion groups and of the Berkeley hydrogen bubble chamber group¹⁶ for scattering and captures of K^- -mesons on free protons have been collected, summarized and combined with the data of this paper. About $\frac{2}{3}$ of the emulsion data below 90 MeV came from reference 2, and about $\frac{2}{3}$ of the emulsion data from 90-140 MeV came from reference 4. This paper contributes about

TABLE III. K^- -meson free proton scattering events.

Event No.	Incident K^- energy (MeV)	K^- scattering angle, θ , in c.m. (deg)
1239	8	153
325	21	88
113 ^a	32	133
403	34	151
64 ^a	35	112
350	49	94
624	55	91
544	59	105
740	80	45
65 ^a	106	23
2040	117	10
2189	119	17
655	131	35
1227	135	169
663	139	41
2074	257	79
2220	286	17
2287	264	49
2282	162	84
2265	292	10

^a These three events were previously reported in reference 1.

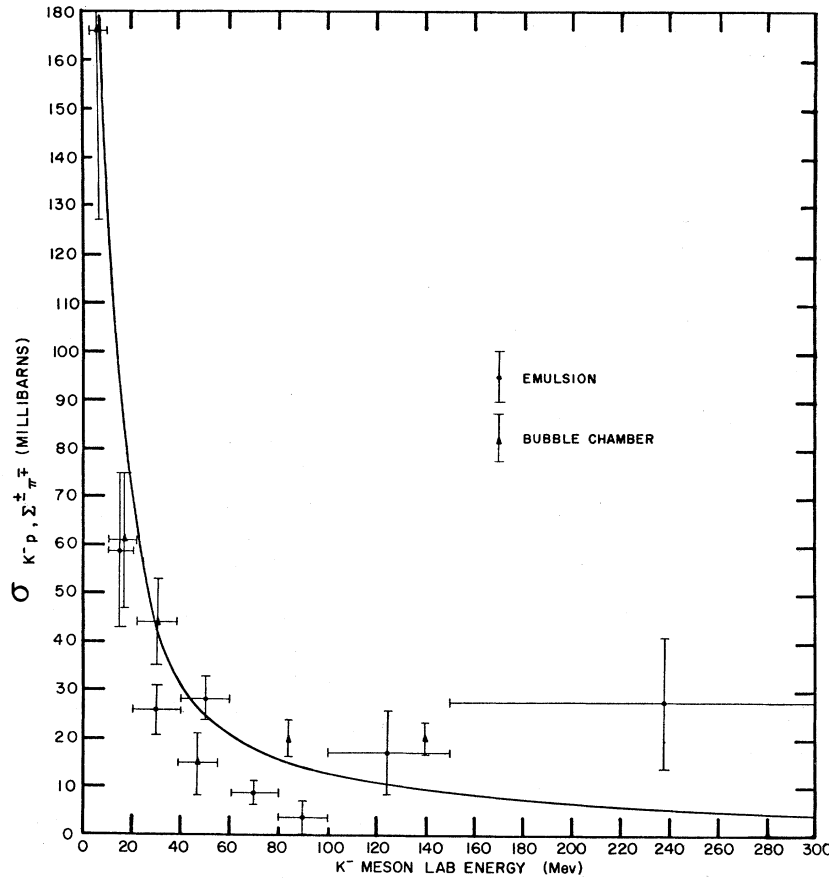


FIG. 2. Plot of the published data for the K^- -meson free proton capture cross section to give a charged Σ hyperon and a charged π meson versus the K^- -meson laboratory kinetic energy. Superimposed on the data is the curve for $\pi\lambda^2/2$, where λ is the K^- -meson wavelength in the center-of-mass system divided by 2π .

$\frac{1}{3}$ of the emulsion data from 90–140 Mev and all the data from 140–300 Mev. The total elastic scattering cross section as a function of the K^- -meson energy appears in Fig. 1. The total cross section for capture to give $\Sigma^+\pi^-$ plus $\Sigma^-\pi^+$ appears in Fig. 2. The curve for $\pi\lambda^2$ is plotted in Fig. 1 and that for $\pi\lambda^2/2$ in Fig. 2. λ is the K^- -meson wavelength in the center-of-mass system divided by 2π . The main features of the (K^-p , K^-p) data are the possible peak or leveling in the cross

section at about 30 Mev, a sharp decrease to about 40 mb and then a fairly flat curve to 300 Mev. It is important that more data be obtained in the region of 30 Mev. On the other hand, the (K^-p , $\Sigma^{\pm}\pi^{\mp}$) cross section, 165 mb at 6 Mev, decreases rapidly to a minimum of about 20 mb at 60 Mev and is then fairly constant to the highest energies. More data is necessary to determine the detailed energy dependence at higher energies.

TABLE IV. K^- -meson free proton capture events.

Event No.	Incident K^- -meson energy (Mev)	π -meson emission angle in c.m. (deg)	Hyperon ^b identity
133 ^a	0.1	...	$\Sigma^-(p)$
662	7	146	$\Sigma_{F^+}^+(p)$
124	112	77	$\Sigma^-(\sigma_3)$
632	113	103	$\Sigma_{R^+}^+(\pi)$
2270	235	126	$\Sigma_{F^{\pm}}^{\pm}(\pi^{\pm})$
2302	270	133	$\Sigma_{F^-}^-(\pi^-)$
2018	280	87	$\Sigma_{F^+}^+(p)$
2037	302	142	$\Sigma_{F^{\pm}}^{\pm}(\pi^{\pm})$

^a This event was previously reported in reference 21.

^b The symbol following the Σ describes the capture star. p signifies no prongs and σ_3 signifies 3 prongs. Sub "F" or "R" indicates a decay in flight or at rest, respectively. (π) or (p) identifies the observed prong as a π meson or a proton.

A plot of the number of events versus $\cos\theta_{c.m.}$ is shown in Fig. 3 for the reaction (K^-p , K^-p). Data are divided into the energy regions <50 , 50–100, and 100–300 Mev. This summary shows no statistically significant asymmetries, in agreement with previously published work,^{2,3,4,11,12} except at energies above 100 Mev where the ratio of forward-to-backward scattering of K^- mesons is 13/2.

No attempt will be made here to explain the energy and angular dependence of the K^-p scattering and capture cross sections. Rather, the reader is referred to the recent theoretical papers which apply a phase-shift analysis²⁹ or a resonance theory³⁰ to explain K^- -interactions.

²⁹ J. D. Jackson, D. G. Ravenhall, and H. W. Wyld, Jr., *Nuovo cimento* 9, 834 (1958); R. H. Dalitz, *1958 Annual International Conference on High-Energy Physics at CERN*, edited

4. K^- -MESON INTERACTIONS ON BOUND NUCLEONS

The study of K^- -meson interactions in flight on nucleons bound in nuclei is of considerable interest because the interactions with neutrons can be studied. In order to understand the K^- interactions with bound nucleons and to determine the energy dependence of the capture and scattering processes it is necessary to have a knowledge of many different properties of the nucleus. The nuclear and Coulomb potentials, the interactions of the reaction products, the internal momentum of the capturing nucleon, and the position of the capture in the nucleus all influence the observable data. Conversely, if the fundamental capture and scattering processes were well known the K^- interactions on nuclei could be used to study the properties of nuclei. An attempt will be made to emphasize the features that are most important in the scattering and capture processes. The model²⁰⁻²² previously used to explain the captures of K^- mesons at rest will be extended to the interactions in flight.

The interaction mean free path in emulsion for K^- mesons is given as a function of energy in Fig. 4. All

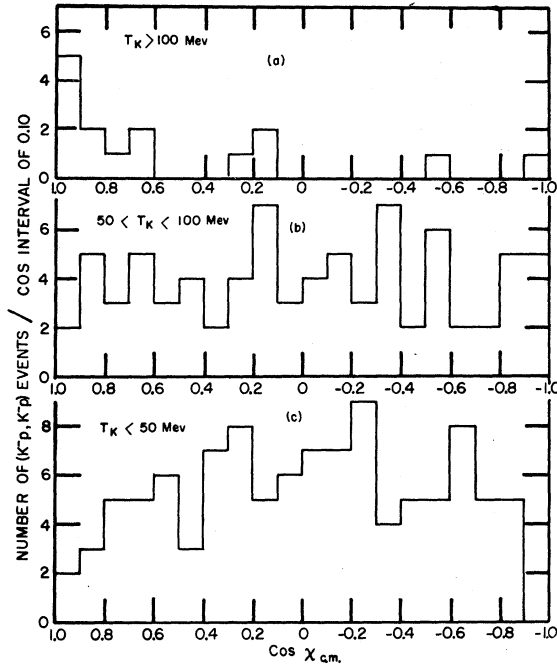


FIG. 3. Plot of the published emulsion data for the number of K^- -meson free proton scattering events versus the cosine of the scattered K^- -meson angle, $\chi_{c.m.}$, in the center-of-mass system. The top graph includes data for $T_K > 100$ Mev, the middle for $50 < T_K < 100$ Mev, and the bottom for $T_K < 50$ Mev. T_K is the K^- -meson kinetic energy in the laboratory system.

by B. Ferretti (CERN Scientific Information Service, Geneva, 1958), p. 188; R. D. Hill, Technical Report No. 7, Office of Naval Research, March, 1959 (unpublished); J. C. Jackson and H. W. Wyld, Jr., Phys. Rev. Letters 2, 355 (1959).

³⁰ P. T. Matthews and A. Salam, Phys. Rev. Letters 2, 226 (1959).

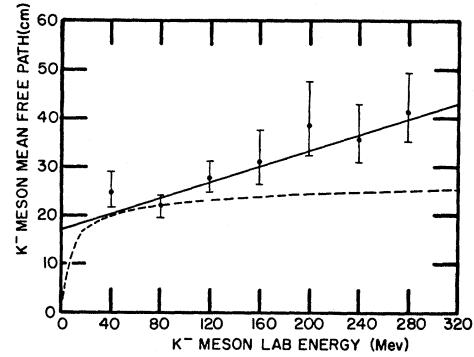


FIG. 4. Plot of the K^- -meson mean free path versus the K^- -meson laboratory energy. All interactions with emulsion nuclei, except hydrogen, are included in which there was an observable energy loss. The dashed curve is a plot of Eq. (7). The solid line is a fit of Eq. (8) to the data.

captures are included which give charged particles, recoils, or blobs. In addition, elastic scatters from light nuclei in which there is an observable recoil are included as well as inelastic scatters where the K^- meson escapes from the capture nucleus with observable prongs, recoils, or blobs. Captures and scatters on free protons and scatters on nuclei which show no observable energy loss are *not* included. The observed K^- -meson track length is shown as a function of the K^- -meson energy in Fig. 5. 56.6 meters of track below 150 Mev and 45.7 meters above 150 Mev were followed.

The dotted curve in Fig. 4 is a plot of the mean free path as calculated from

$$\Lambda(T_K) = \frac{1}{\pi \sum n_i [\lambda(T_K) + r_i]^2}, \quad (7)$$

where T_K is the laboratory K^- -meson kinetic energy, n_i is the number of nuclei/cm³ of a particular element of the emulsion, and r_i is calculated from $r_i = 1.4 \times A_i^{1/3} \times 10^{-13}$ cm. A_i is the atomic number of the i th element. Emulsion hydrogen nuclei are not included in this calculation. This curve does not fit the data. Good agreement is obtained from the least-squares fit of the data to the line

$$\Lambda(\text{cm}) = (17.2 \pm 3.4) + (0.081 \pm 0.027) T_K, \quad (8)$$

which is plotted as a solid line in Fig. 4. The mean free path more than doubles in going from an extrapolated 17.2 ± 3.4 cm at 0 Mev to 41.5 ± 4.4 cm at 300 Mev. At the highest energy the mean free path is 50% longer than the 28 cm which corresponds to nuclear area in emulsion.

Since the nucleus is apparently becoming transparent to K^- mesons at high energies, we have applied the "optical model" of Fernbach, Serber, and Taylor.³¹ The absorption cross section for high-energy neutrons

³¹ S. Fernbach, R. Serber, and T. B. Taylor, Phys. Rev. 75, 1352 (1949).

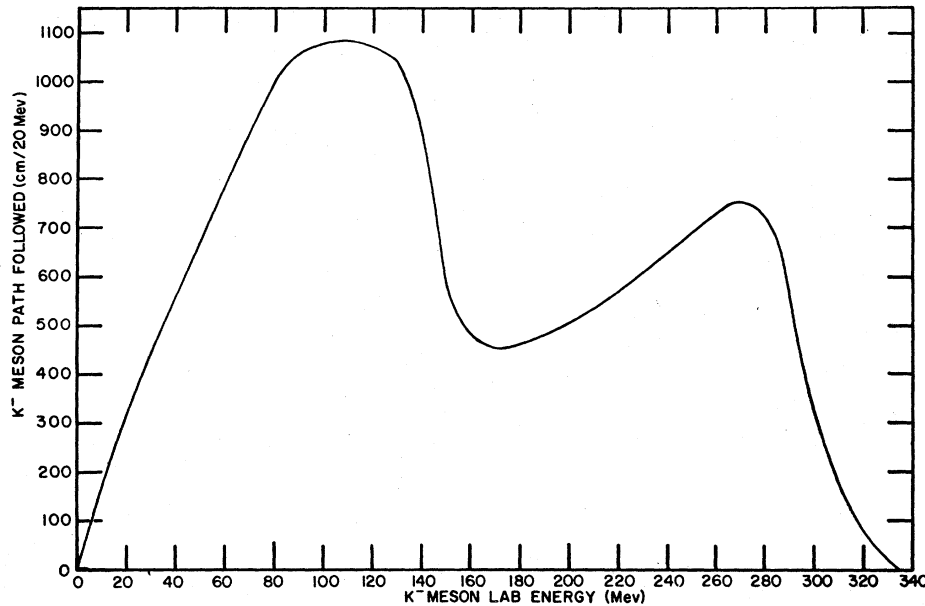


FIG. 5. Plot of the total K^- -meson path followed in this experiment versus the K^- -meson laboratory kinetic energy.

is given by

$$\sigma_i = \pi R_i^2 \{ [1 - (1 + 2KR) e^{-2KR_i}] / 2K^2 R_i^2 \}, \quad (9)$$

where $R_i = r_i + \lambda$ is the effective nuclear radius of the interaction. K is the absorption coefficient for neutrons in nuclear matter. The value of the mean free path in emulsion can be expressed as

$$\Lambda_e = 1 / \sum_i n_i \sigma_i, \quad (10)$$

where σ_i is the absorption cross section of the i th element in nuclear emulsion. Equations (9) and (10) are solved simultaneously for $K \equiv 1/\Lambda_N$ in terms of the measured Λ_e (Fig. 4). These experimental values of Λ_N are shown in Fig. 6.

The capture cross section per nucleon has been estimated as a function of energy from the (K^-p , $\Sigma^\pm \pi^\mp$) cross section (Fig. 2). The scattering cross section has been taken as $\frac{2}{3}$ of the (K^-p , K^-p) cross section (Fig. 1).³¹ These crude estimates assume that the neutron cross sections are equal to the proton cross sections and they neglect the K^-p reactions which lead to neutral secondaries. The mean free path for K^- mesons in the nucleus, which is calculated from these cross sections, is plotted as the solid curve in Fig. 6. The agreement is reasonable and indicates that the increase with energy of the K^- -meson mean free path in nuclear emulsion can be quantitatively explained in terms of the decreasing nucleon cross section.

A. K^- -Meson Inelastic Scattering

Below 100 Mev only about 2% of the K^- mesons undergo inelastic scattering. One of the interesting results of this experiment is the increase in inelastic scattering that appears at higher energies. The ratio of the number of inelastic scattering events to the number

of interactions on emulsion nuclei is plotted against the K^- -meson kinetic energy in Fig. 7. In order for a K^- interaction to fall into this category, an energy loss of more than 10 Mev must be observed at the interaction point. The rise of the fraction of inelastic events to about 15% at 150 Mev is quite marked. In fact, several tracks were observed where the K^- meson inelastically scattered twice before coming to rest.

The decrease in the interaction cross section with increase in K^- -meson energy which was demonstrated in Fig. 4 is related to the increase in the fraction of

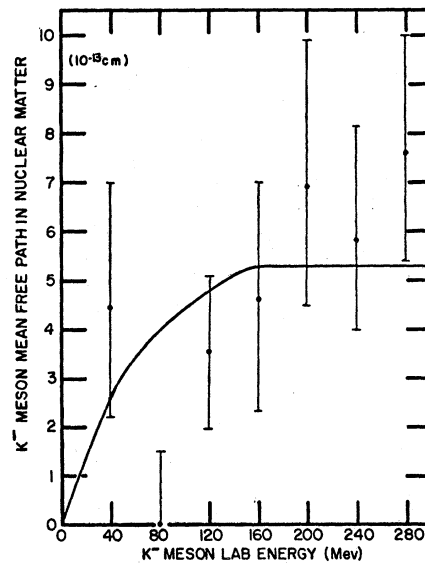


FIG. 6. Plot of the K^- -meson mean free path in nuclear matter versus the K^- -meson kinetic energy. The plotted points were obtained from Eqs. (9) and (10). The curve was obtained by applying the "optical model" of Fernbach, Serber, and Taylor, reference 31. See text.

inelastic K^- -meson scattering above 100 Mev. Here, the nucleus starts to become partially transparent to the K^- mesons. Some scatter from nucleons inside the nucleus and then escape. Above 80 Mev, the combined bubble chamber and emulsion data for K^- meson scatters and captures on free protons (see Fig. 1) indicate that the scattering cross section of about 40 mb is twice the capture cross section (20 mb) to give charged hyperons. The higher scattering-to-capture ratio leads to the observed increase in the inelastic scattering from nuclei.

An event in which a short recoil prong was observed at the scattering point and in which the K^- meson lost little or no energy was interpreted as a K^- -meson elastic scattering from a light nucleus of carbon, nitrogen, or oxygen. These events occur in about 2% of the interactions. In order to obtain the corrected number of K^- meson captures the inelastic and light nuclei scattering events were subtracted from the total number of K^- interactions. The fraction of events in each of the categories, Σ hyperon, π meson, Σ - π pairs, hyperfragments, stable prongs only, and no observable prongs is obtained by dividing the number of events in each category by the corrected total.

B. $\Sigma^0\pi^0$, $\Lambda^0\pi^0$, and \bar{K}^0n Reactions

The fraction of $K^-(\rho)$ events remains approximately constant (10% of the total) from 20 to 300 Mev. In these events the K^- mesons stop in flight with the emission of no charged prongs. These may be examples of K^- meson captures on free protons via the reactions $\Sigma^0\pi^0$, $\Lambda^0\pi^0$, and \bar{K}^0n , or they may be examples of the same reactions which take place on bound protons in nuclei in which no charged prongs are emitted. It is also possible that such events result from the interactions inside the nucleus of the charged prongs from the primary reactions $\Sigma^+\pi^-$, $\Sigma^-\pi^+$, $\Sigma^-\pi^0$, $\Sigma^0\pi^-$, and $\Lambda^0\pi^-$ in such a manner that no charged prongs are emitted.

The observed \bar{K}^0n cross-section peaks at about 15 mb at 30 Mev³² and drops to 5 mb at 90 Mev. At 80 and 140 Mev the sum of the $\Sigma^0\pi^0$ and $\Lambda^0\pi^0$ cross sections is 15 mb.¹⁶ If all the $K^-(\rho)$ events below 150 Mev were

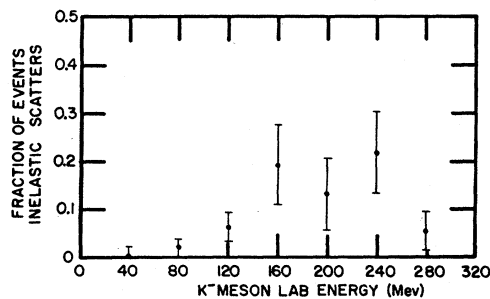


Fig. 7. Plot of the fraction of events which are inelastic scatters versus the K^- -meson laboratory kinetic energy.

³² P. Eberhard, A. H. Rosenfeld, F. T. Solmitz, R. D. Tripp, and M. B. Watson, Phys. Rev. Letters 2, 312 (1959).

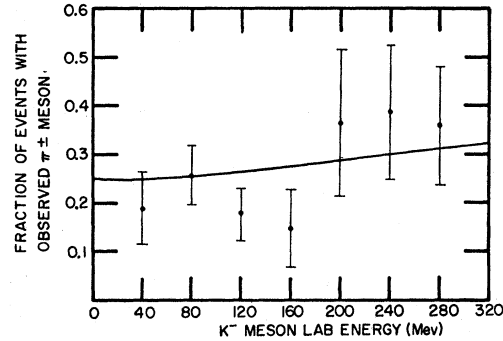


Fig. 8. Plot of the fraction of events with observed charged π mesons versus the K^- -meson laboratory kinetic energy. The solid curve is a plot of Eq. (9).

free proton captures or charge exchanges the cross section would be 110 mb which is much too high; therefore, most of the low-energy $K^-(\rho)$ events must be attributed to captures on bound nucleons in nuclei. As the K^- -meson kinetic energy is raised, an increasing amount of energy is given to the capturing nucleus which increases the probability for charged particle emission. At K^- -meson energies above 150 Mev a larger fraction of the $K^-(\rho)$ events may be captures on free protons. If all $K^-(\rho)$ events between 150 and 300 Mev are classified as free proton events an upper limit to the sum of the K^- -meson free proton cross section for the reactions $\Sigma^0\pi^0$, $\Lambda^0\pi^0$, and \bar{K}^0n in this energy region is found to be 45 ± 16 mb.

C. π Mesons

Although a careful examination was made of the charged particles from each K^- -meson interaction, no example was seen of an inelastic scatter with the production of a π meson. This is not surprising in view of the fact that the K^- meson has a large cross section for the competing $\Sigma\pi$ capture reactions. These $\Sigma\pi$ capture reactions are forbidden to the K^+ meson by conservation of strangeness. Three examples of π production have been seen from K^+ inelastic interactions in 331 m of track in the energy region of 200–400 Mev.³³ π production from K^- -meson inelastic scattering has also been seen at 760 Mev.¹⁴ The number of K^- -meson captures which give π mesons, divided by the total number of events in which the K^- meson is captured, is plotted versus the K^- -meson kinetic energy in Fig. 8. The fraction of K^- -meson captures in which π mesons are observed is 0.21 ± 0.03 at K^- -meson energies of 20–150 Mev and is 0.33 ± 0.06 for energies of 150–300 Mev. This increase can be explained in terms of the known interaction cross sections for π mesons in nuclear matter.

The solid line that appears in Fig. 8 is a plot of the

³³ E. Helmy, J. H. Mulvey, D. J. Prowse, and D. H. Stork, Phys. Rev. 112, 1793 (1958). 1958 Annual International Conference on High-Energy Physics at CERN (CERN Scientific Information Service, Geneva, 1958), p. 174.

calculated fraction of events, f_{es} , which give charged π mesons that escape from the nucleus. It is obtained from the expression

$$f_{es} = \frac{2}{3} [f_t + (1 - f_t)f_{ie}]. \quad (11)$$

f_t is the fraction of π mesons that do not interact in leaving the nucleus and is obtained from the π -meson escape formula which is applicable for the case in which the π mesons are produced uniformly throughout the nucleus.³⁴ The total mean free path in nuclear matter was calculated from a phase-shift analysis of π -meson scattering data.³⁵ f_{ie} is the fraction of inelastically scattered π mesons. It is obtained from experimental data for π -meson interactions in nuclear emulsion. A summary of the inelastic scattering data by Blau and Caulton³⁶ gives values for f_{ie} of 0.03 ± 0.02 , at 40 Mev, 0.10 ± 0.03 at 70 Mev, 0.19 ± 0.04 at 105 Mev, 0.22 ± 0.03 at 135 Mev, 0.38 ± 0.08 at 210 Mev, and 0.38 ± 0.06 at 500 Mev. The fraction, $\frac{2}{3}$, in the formula comes from the application of charge independence to a nucleus with equal numbers of protons and neutrons. The total number of charged π mesons produced is equal to twice the number of π^0 mesons. The π -meson energies are calculated from the K^- -meson free nucleon capture (Σ, π) reactions. If the angular distribution of the produced π mesons is uniform in the center-of-mass system, the number of π mesons per unit π -meson laboratory kinetic energy is approximately constant between the minimum and maximum allowed energies. The fractions, f_t and f_{ie} , were averaged over the allowed π -meson energy regions and Eq. (11) was evaluated as a function of the K^- -meson energy. The

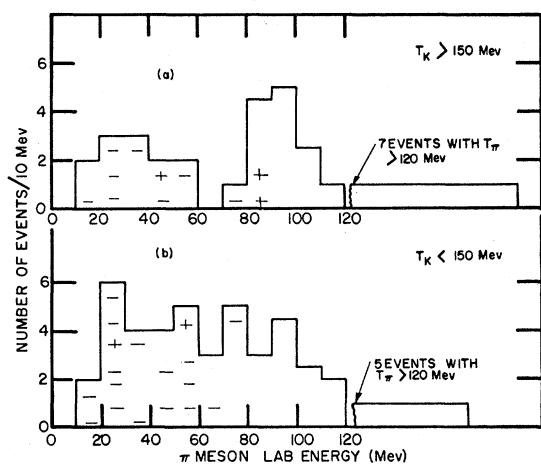


FIG. 9. Plot of the number of events in which π^\pm mesons are emitted versus the π -meson laboratory kinetic energy. In (a), $T_K > 150$ Mev and in (b), $T_K < 150$ Mev. In (a) there are 7 events with $T_\pi > 120$ Mev which are plotted as 1 event for each of 7 consecutive energy intervals. In (b) the same is done for 5 events.

³⁴ K. A. Brueckner, R. Serber, and K. M. Watson, Phys. Rev. **84**, 258 (1951).

³⁵ R. M. Frank, J. L. Gammel, and K. M. Watson, Phys. Rev. **101**, 891 (1956).

³⁶ M. Blau and M. Caulton, Phys. Rev. **96**, 150 (1954).

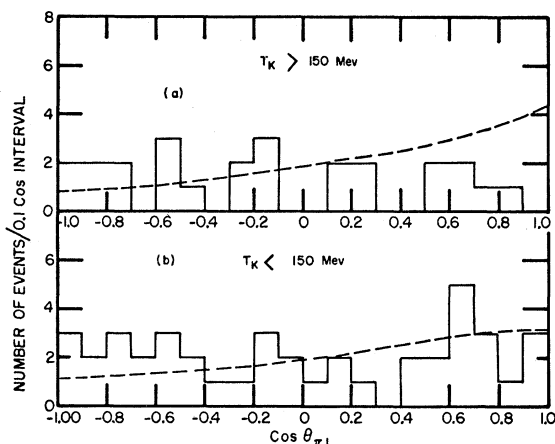


FIG. 10. Plot of the number of events in which π^\pm mesons are emitted versus the cosine of the laboratory angle of emission, $\theta_{\pi L}$. In (a), $T_K > 150$ Mev and in (b), $T_K < 150$ Mev. The dashed lines show the distributions expected if the π mesons are produced isotropically in the center-of-mass system of the nucleon and the K^- meson and if the π mesons escape from the nucleus with their angles unchanged.

curve in Fig. 8 shows a gradual increase in f_{es} with the K^- -meson energy in reasonable agreement with the data.

The calculation also gives the result that 50% of the observed π mesons from K^- -meson interactions between the energies of 20 and 150 Mev and 60% of the observed π mesons from K^- mesons between 150 and 300 Mev were inelastically scattered before leaving the nucleus. Contrary to what is observed for K^- captures at rest there is little correlation between the energies of the π mesons at production in the nucleus and their observed energies outside the nucleus. This was emphasized by the Berne group⁹ for interactions of K^- -mesons with energies from 20 to 150 Mev. The same is true for π mesons from interactions of K^- mesons with energies from 150 to 300 Mev. This is because π mesons near the 180 Mev ($\frac{3}{2}, \frac{3}{2}$) resonance interact very strongly with nuclear matter. The experimental result of Fig. 9 for the energies of the observed π mesons demonstrates that most of the observed π mesons are at low energies and therefore have undergone inelastic scattering before leaving the nucleus. Only $21 \pm 7\%$ and $32 \pm 10\%$ of the π mesons for the low- and high-energy K^- -meson intervals, respectively, have energies above 100 Mev. These experimental values, however, are still substantially larger than the same experimental fraction, $7 \pm 2\%$, for π mesons from K^- -meson captures at rest.^{9,12} The fact that most of the π meson- Σ hyperon events from K^- captures in flight are accompanied by additional prongs, contrary to what is observed when K^- mesons at rest are captured by nuclei, supports the inelastic collision viewpoint.

The angular distributions of the π mesons with respect to the directions of the incident K^- mesons are shown in Figs. 10 (a) and (b). The curves shown on

the graph give the angular distributions expected for K^- -nucleon collisions if the production is isotropic in the center-of-mass system. In the laboratory system there should be a definite forward-backward asymmetry of a factor of about 2 due to the center-of-mass transformation. Since the π mesons, even for the K^- -meson energy interval of 150–300 Mev, show no such forward-backward asymmetry, and since the effect should be statistically observable, we again conclude that most of the π mesons that get out of the nucleus have been scattered and consequently have not preserved their original directions.

The π^-/π^+ ratio in the K^- -meson energy interval of 20–150 Mev is 18/3 and in the interval of 150–300 Mev is 8/3. The ratio over the whole energy interval is $4.3_{-1.7}^{+3.1}$. This value is in good agreement with the ratios, 3.5 ± 0.6 , of the Berne group,⁹ 3.9 ± 0.7 of the K -stack collaboration,¹² and 3.3 ± 0.9 that were obtained by the authors from K^- -meson interactions at rest on nuclei.²² It is lower than the value $45/4 = 11.4^{+12}$ that was obtained by the Berne group⁹ for K^- energies of 20–150 Mev. Because of the agreement with the ratio for K^- captures at rest there is no evidence, here, that the production ratios for captures on nuclei at K^- -meson energies from 20–300 Mev are different than for K^- -mesons at rest. It is kept in mind that the captures "at rest" on nuclei should be similar to low-energy captures "in flight" on free nucleons because of the nucleon momentum distribution in the nucleus.

D. Σ Hyperons

a. Σ Hyperon Energy Distributions

It is of interest to determine whether the K^- mesons are captured at the energies they strike the nuclei or whether they are greatly reduced in energy by scattering before being captured. Because the π mesons, themselves, interact so vigorously before leaving nuclei their observed energies are not very sensitive to the K^- -meson energies at capture. The Σ hyperons, since they are 8 times as heavy as the π mesons, are more likely to retain their original directions in nuclear matter. In escaping from the nucleus many hyperons that are not trapped will also retain their initial energies modified by the nuclear and Coulomb potentials.

The expected Σ -hyperon kinetic energies in Mev are calculated from

$$T_{\Sigma^-} = T_{\Sigma^- F} - 45, \quad (12)$$

$$T_{\Sigma^+} = T_{\Sigma^+ F} - 25. \quad (13)$$

$T_{\Sigma F}$ is the Σ -hyperon energy calculated from the free proton kinematics for a given K^- -meson energy and Σ -hyperon angle. For energies above 50 Mev the K^- -meson nucleon relative momentum is determined primarily by the K^- -meson energy. Although the nucleon momentum distribution will broaden the Σ -hyperon energy distribution, it is neglected here. The sum of the binding and excitation energies,

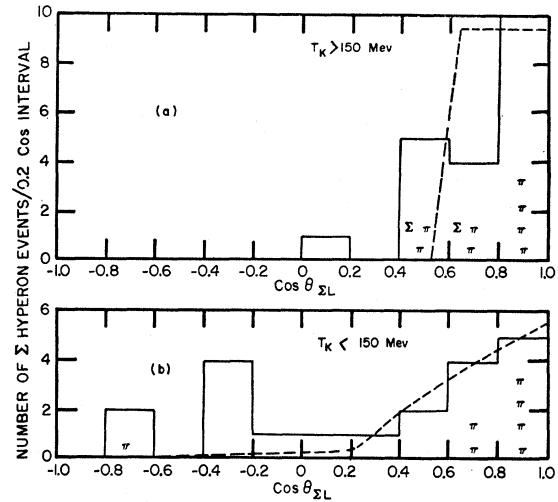


FIG. 11. Plot of the number of Σ^\pm hyperons versus the cosine of the Σ -hyperon laboratory angle, $\theta_{\Sigma L}$. In (a), $T_K > 150$ Mev and in (b), $T_K < 150$ Mev. A " π " designates an event in which there was a charged π meson associated with the Σ hyperon. A " $\Sigma\pi^-$ " designates an event in which both a Σ^- hyperon and a π^- meson were emitted. The dashed curves are the distributions expected for isotropic emission of the Σ hyperons in the center-of-mass system of the K^- meson and the nucleon if the Σ -hyperon angle is unchanged in escaping from the nucleus.

about 20 Mev, is furnished primarily at the expense of the π -meson energy and is also neglected. The Σ -hyperon potentials, however, are included because a nuclear potential of 35 Mev and a Coulomb potential of 10 Mev are comparable to the Σ -hyperon energies, particularly at low K^- -meson incident energies.

The observed energies of the Σ hyperons which were accompanied by π mesons are in good agreement with the above calculation. Six of the hyperons had energies above and seven below the energies calculated. On the other hand, among the Σ hyperons which were not associated with π mesons, there were 3 above and 19 below the calculated energies. Many of the hyperons in this latter group, therefore, apparently suffered appreciable energy loss before escaping from the nucleus. The Σ hyperons associated with π mesons probably originated from captures near the edge of the nucleus while those without π mesons were probably produced farther in. In the latter case the π mesons were captured and most of the Σ hyperons were scattered inelastically. It should be pointed out that these Σ hyperons did not originate by captures on 2 nucleons, each of which gives a hyperon and a nucleon. The hyperon kinetic energies here would have been even higher than for the single nucleon captures, in greater disagreement with the data.

Additional evidence for the Σ -hyperon K^- -meson correlation is found in the Σ -hyperon laboratory angular distribution. If the production is isotropic in the center-of-mass system, the distribution in the laboratory system is proportional to $d(\cos\theta_{\Sigma C})/d(\cos\theta_{\Sigma L})$, where $\theta_{\Sigma C}$ and $\theta_{\Sigma L}$ are the Σ -hyperon angles

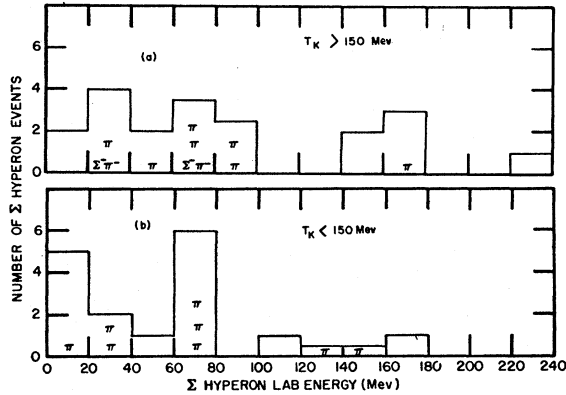


FIG. 12. Plot of the number of Σ^\pm hyperons versus the Σ -hyperon laboratory kinetic energy. In (a), $T_K > 150$ Mev and in (b), $T_K < 150$ Mev. A “ π ” represents an event in which an observed π meson accompanies the Σ hyperon. A “ $\Sigma\pi^-$ ” represents an event in which both a Σ^- hyperon and a π^- meson were emitted.

relative to the incident K^- meson in the center-of-mass and laboratory systems, respectively. In order to predict the angular distribution it is necessary to fold in the probability for producing and observing Σ hyperons at the observed energies. The predicted curves and the experimental data are shown in Figs. 11 (a) and (b). The curves for $T_K < 150$ Mev and > 150 Mev are normalized to the number of events with $\cos\theta_{\Sigma L} > 0.0$ and > 0.40 , respectively. The Σ hyperons with angles outside these regions were probably scattered before escaping from the nucleus. The fits of the predicted curves to the data, for Σ hyperons accompanied by π mesons, show that the Σ -hyperon angles of emission are indeed correlated with the incident K^- -meson energies. A fair fit is also obtained for those Σ hyperons not accompanied by π mesons for $T_K > 150$ Mev but for $T_K < 150$ Mev the fit is poor.

A “ π ” symbol in a box of Figs. 11 (a) and (b) designates a Σ hyperon that is accompanied by a π meson. The 2 events with “ $\Sigma\pi^-$ ” are cases where both a Σ^- hyperon and a π^- meson came out of the same capture event. This type of event is extremely rare in K^- captures at rest.²¹ These two events are interpreted as cases where either a Σ^0 hyperon or a π^0 meson underwent charge exchange. Because of the low π^- meson kinetic energy in both cases, they are thought to be examples of π^0 charge exchange according to the reaction



The Σ -hyperon energy distributions for $T_K > 150$ Mev and < 150 Mev are given in Figs. 12 (a) and (b). The “ π ” and “ $\Sigma\pi^-$ ” have the same significance as in Figs. 11 (a) and (b). Again there is no evidence that Σ hyperons not accompanied by π mesons have higher energies than those which are accompanied by π mesons. Consequently, there is no evidence for a significant contribution from 2-nucleon capture of a K^- meson to give a fast hyperon and a fast nucleon.

This conclusion was previously obtained by the Berne group.⁹ It can be seen from Fig. 12 however, that the Σ -hyperon energies do extend to higher values for the K^- -meson captures in flight than for K^- -meson captures at rest.^{10,12,21,22} This is further evidence that the incident K^- meson and the Σ -hyperon energies are correlated.

b. Observed Number of Σ Hyperons

Along with the increase in the K^- -meson escape probability at high K^- -meson kinetic energies there is also expected an increase in the Σ -hyperon escape probability on the basis of the proposed model. The greater energy available in the K^- -nucleon system for higher energy K^- mesons will result in higher energy Σ hyperons. Because of the decrease in the amount of trapping in the nuclear potential with an increase in the Σ -hyperon energies, the number of Σ hyperons which escape the nucleus should increase as the K^- -meson kinetic energy is increased. This is true if the production and interaction cross sections do not change appreciably. It is estimated that the fraction of trapped Σ^+ hyperons decreases from 50% at a K^- -meson energy of 50 Mev to 10% at 300 Mev and the fraction of trapped Σ^- hyperons decreases from 70% to 15% in the same energy interval.

The position of the capture point in the nucleus is also important in determining the fraction of Σ hyperons that escape. It was pointed out in Sec. 4A that the nucleus starts to become transparent to K^- mesons at about 150 Mev. Below this energy the K^- mesons are stopped primarily on the front side of the nucleus. Since the Σ hyperons are usually emitted at small forward lab angles, they then have to penetrate the rest of the nucleus before escaping. If the interaction cross section for Σ hyperons were not energy dependent, more of those produced by low-energy K^- mesons than produced from uniformly captured K^- mesons would interact in flight.

For K^- captures at energies below 150 Mev, it is estimated that 60% of all Σ hyperons are trapped and an additional 20% are captured in flight. If the K^- mesons are captured on the front surface of the nucleus and if the Σ hyperons go forward through the nucleus, these numbers imply a capture mean free path of $10_{-3}^{+8} \times 10^{-13}$ cm and a cross section of 7 ± 4 mb per

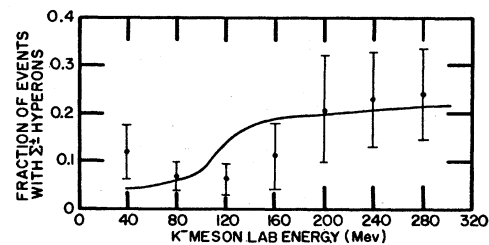


FIG. 13. Plot of the fraction of events with observed Σ hyperons versus the K^- -meson laboratory kinetic energy. The curve is the calculated fraction (see text for explanation).

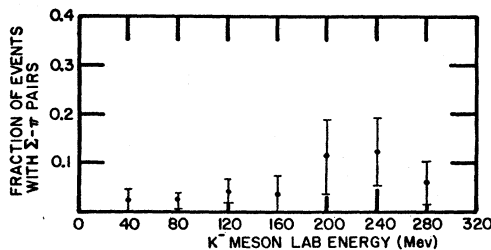
TABLE V. Fraction of events in which Σ^\pm hyperons, π^\pm mesons, and $\Sigma^\pm\pi^\mp$ pairs escape from the nucleus.

Particles that escape from nucleus	Fraction of events		K-stack collaboration ^a $T_K=0$ Mev	Berne ^b $20 \leq T_K \leq 150$ Mev
	$20 \leq T_K \leq 150$ Mev	$150 \leq T_K \leq 300$ Mev		
(1) Σ^\pm hyperon	0.11 ± 0.03	0.21 ± 0.05	0.18 ± 0.02	0.08 ± 0.02
(2) π^\pm meson	0.21 ± 0.03	0.33 ± 0.06	0.31 ± 0.02	0.22 ± 0.03
$1.32 \times (1) \times (2)$	0.030 ± 0.009	0.091 ± 0.026	0.074 ± 0.009	0.024 ± 0.007
(3) $\Sigma^\pm\pi^\mp$	0.042 ± 0.017	0.094 ± 0.034		0.020 ± 0.008

^a See reference 12.^b See reference 9.

nucleon in the nucleus. For K^- -meson captures at energies from 150 to 300 Mev, it is estimated that 15% of all Σ hyperons are trapped and an additional 45% are captured in flight. Using the facts that the K^- mesons in this energy range are probably captured uniformly throughout the nucleus and that the Σ hyperons then go forward, a capture mean free path of $(4 \pm 2) \times 10^{-13}$ cm and a cross section of 16 ± 6 mb per nucleon in the nucleus are obtained. Because a Σ^- hyperon can be captured only by a proton and a Σ^+ hyperon can be captured only by a neutron the above listed Σ -hyperon nucleon cross sections may be underestimated by a factor of as much as two for the case where the direct capture cross sections are much greater than the scattering cross sections. Since these cross sections do not differ appreciably from the previously obtained value of 11.6^{+7} mb per nucleon for Σ hyperons from K^- captures at rest,²² this latter value, independent of Σ -hyperon energy, will be used for subsequent calculations.

With reasonable production ratios^{2,16,37} for $\Sigma^- \pi^+$: $\Sigma^+ \pi^-$: $\Sigma^0 \pi^0$: $\Sigma^0 \pi^-$: $\Sigma^- \pi^0$: of 1:1:1:0.4:0.4 (the fraction of $\Lambda^0 \pi$ reactions in the primary capture process is considered small) the fraction of events in which the Σ^\pm hyperons escape, $f_c f_{nt} f_{nf}$, is calculated and plotted along with the experimental data in Fig. 13. f_c is the fraction of primary events in which charged Σ hyperons are produced, f_{nt} is the fraction of Σ hyperons not trapped, and f_{nf} is the fraction of Σ hyperons that are not captured in flight. The data show the predicted increase with K^- -meson energy.

Fig. 14. Plot of the fraction of events with an observed $\Sigma^\pm\pi^\mp$ pair versus the K^- -meson laboratory kinetic energy.³⁷ M. F. Kaplon, 1958 Annual International Conference on High-Energy Physics at CERN (CERN Scientific Information Service, Geneva, 1958), p. 176.

c. Σ^-/Σ^+ Ratio

The experimental Σ^-/Σ^+ hyperon ratios for K^- captures from 20–150 Mev and 150–300 Mev are 1.8 ± 0.8 and 0.9 ± 0.4 , respectively, in satisfactory agreement with the production ratios given above. The measured ratio from emulsion and bubble chamber data for K^- captures on free protons starts at 2 for captures at rest, is uncertain from 0 to 20 Mev, and then approaches 1 at higher energies. K^- captures at rest on bound nucleons primarily occur in the transition region where the production ratios are uncertain. At K^- -meson energies above 20 Mev the Σ^-/Σ^+ hyperon ratio for bound nucleons should approach the value for the free nucleon captures as fewer Σ hyperons are trapped by the nuclear and Coulomb potentials. Additional data are needed to study the variation in the Σ^-/Σ^+ hyperon ratios with K^- -meson energy.

Because of the larger individual escape probabilities of the π mesons and the Σ hyperons at K^- meson energies greater than 150 Mev, the fraction of cases in which a Σ hyperon- π meson pair escapes from the nucleus is also increased. A plot of the fraction of events with $\Sigma^\pm\pi^\mp$ pairs as a function of the K^- -meson energy is shown in Fig. 14. The fraction of $\Sigma^\pm\pi^\mp$ pairs appears to increase with K^- -meson energy. A summary of the experimental fractions of events that yield Σ^\pm hyperons, π^\pm mesons, and $\Sigma^\pm\pi^\mp$ pairs is given in Table V. The data of the Berne group⁹ for K^- -meson energies of 20–150 Mev and of the K-stack collaboration¹² for captures at rest have also been included for comparison. From the production ratios assumed in paragraph b above, the fraction of events with $\Sigma^\pm\pi^\mp$ pairs that escape is given by 1.32 times the product of the fraction of events with Σ^\pm that escape times the fraction of events with π^\pm that escape. From Table V it may be seen that this product is in agreement with the fractions of $\Sigma^\pm\pi^\mp$ pairs observed at various energies.

d. Hyperfragments

Hyperfragments were observed in 3.5 ± 1.3 and $6.3 \pm 2.5\%$ of the events in the K^- -meson energy regions of 20–150 and 150–300 Mev, respectively. The value for the lower energy region is in good agreement with the value of $4.0 \pm 1.0\%$ obtained by the Berne⁹

group. Values of 3.4 ± 0.3^{12} and 4.2 ± 0.9^{10} have been obtained for K^- -meson captures at rest.

5. CONCLUSIONS

Data are presented for K^- -meson interactions and decays at energies of 20 to 300 Mev. The following results have been obtained:

(1) From 33 K^- -meson decays the lifetime was found to be $(1.38 \pm 0.24) \times 10^{-8}$ sec in agreement with the K^+ -meson lifetime of $(1.24 \pm 0.02) \times 10^{-8}$ sec. Examples of each of the decay modes $K_{\mu 2}$, $K_{\mu 3}$, $K_{\pi 2}$, τ , and τ' were identified. The branching ratios are in agreement with those for K^+ mesons. This is the result expected if the K^- meson is the antiparticle of the K^+ meson.

(2) The (K^-p, K^-p) elastic scattering cross section was found to be 35 ± 16 mb and the $(K^-p, \Sigma^{\pm}\pi^{\mp})$ cross section 27 ± 13 mb in the energy region of 150 to 300 Mev. The published data on these two cross sections for energies of 5 to 300 Mev are summarized. The $(K^-p, \Sigma^{\pm}\pi^{\mp})$ cross section is close to $\pi\lambda^2/2$ from 5 to 100 Mev.

(3) The mean free path for K^- -meson captures, inelastic scatters, and elastic scatters on emulsion nuclei, except hydrogen, in which there was an observable recoil can be represented by

$$\Lambda(\text{cm}) = (17.2 \pm 3.4) + (0.081 \pm 0.027)T_K,$$

for energies of 20 to 300 Mev. This increase in the mean free path with K^- -meson energy is explained in terms of the decreasing nucleon cross section.

(4) The fraction of inelastic scatters increases from about 2% at low K^- -meson energies to about 15% at 150 Mev. This effect is additional evidence that the nucleus is becoming transparent to K^- mesons at about 150 Mev.

(5) The increase in the number of Σ hyperons that escape from the nucleus at higher K^- -meson energies is partially due to the decrease in the number of Σ hyperons that are trapped. This effect is consistent with the Σ -hyperon nuclear potential of 35 ± 10 Mev and the Coulomb potential of 10 ± 3 Mev that were previously proposed for explaining K^- -meson captures at rest on bound nucleons.^{21,22} In addition, low-energy K^- mesons are captured near the front of the nucleus such that the Σ hyperons traverse most of the nucleus and a large fraction are captured. At higher energies the K^- mesons interact more uniformly throughout the nucleus and a larger fraction of the Σ hyperons escape.

(6) The observed number, energies, and angles of the π mesons are greatly influenced by their mean free paths for capture and scattering in the nucleus in which they are produced. At π -meson energies near the $(\frac{3}{2}, \frac{3}{2})$ resonance the very strong interaction cross sections

overshadow all other effects and little information is gained from the π -meson energies about the K^- -meson capture mechanism. The π^-/π^+ ratio is $4.3_{-1.7}^{+3.1}$ for K^- captures from 20–300 Mev. It is in good agreement with the corresponding ratios for K^- captures by free protons in bubble chambers and emulsions stacks^{2,15,37} at low energies, and for K^- captures at rest in emulsion.^{21,22} Therefore, there is no evidence, here, that the K^- -meson production ratios are different for energies of 20–300 Mev than for K^- captures at rest on nuclei.

(7) It is difficult to separate the Σ -hyperon interactions with nucleons in the nucleus from the other large effects. One can fit the data of this experiment for $T_K < 150$ Mev with a Σ -hyperon mean free path in nuclear matter of $(10_{-3}^{+8}) \times 10^{-13}$ cm and a cross section of (7 ± 4) mb per nucleon. For $T_K > 150$ Mev the mean free path is $(4 \pm 2) \times 10^{-13}$ cm and the cross section is (16 ± 6) mb per nucleon. This is in agreement with the value of (11_{-6}^{+7}) mb per nucleon obtained previously for Σ hyperons from K^- captures at rest on nuclei.²²

(8) The captures take place predominantly on single nucleons at approximately the energies that the K^- mesons enter the nuclei. For the $\Sigma^{\pm}\pi^{\mp}$ events the correlation of the Σ -hyperon angle and energy with the energy of the incoming K^- meson is good when a one-nucleon capture process is assumed. For those events where a Σ hyperon and no π meson is observed the correlation is not as good and the energies are lower than for the $\Sigma^{\pm}\pi^{\mp}$ cases. Therefore, these Σ hyperons probably scattered inelastically before escaping from the nucleus. Σ hyperons from the 2-nucleon capture processes, which give a Σ hyperon and a nucleon, will have considerably higher energies on the average than those from one-nucleon captures. No example was seen of a K^- capture with the emission of a Σ hyperon and a nucleon whose energies were consistent with a capture by two nucleons. There is no evidence from this experiment that the primary Λ^0 hyperon production is different from K^- -meson captures at rest where the production is low.²²

6. ACKNOWLEDGMENTS

We would like to thank Dr. E. Lofgren and the bevatron crew for their assistance and cooperation in exposing the emulsion stacks used in this experiment. We gratefully acknowledge the use of the 300-Mev K^- -meson beam which was set up primarily through the efforts of Dr. D. H. Stork and Dr. J. H. Mulvey. We are particularly indebted to Miss Patricia Banks, Mrs. Irene Brown, Miss Claudia Crane, Mrs. Theodora Hilliard, Mrs. Beverly Lagiss, Mrs. Emily Muskopf, Mrs. Barbara Sawyer, and Mrs. Elizabeth Wilson for locating the events and for taking measurements.